

# Improvement of Processing and Mechanical Properties of Polyetherimide by Antiplasticization with Resorcinol Bis(diphenyl phosphate)

Evandro M. Alexandrino, Thiago F. da Conceição, Maria I. Felisberti

Institute of Chemistry, University of Campinas (UNICAMP), Campinas 13083-970, Brazil

Correspondence to: M. I. Felisberti (E-mail: misabel@iqm.unicamp.br)

**ABSTRACT:** This article describes the antiplasticization of a commercial polyetherimide ULTEM® series 1000 [poly(bisphenol A-co-4-nitrophthalic anhydride-co-1,3-phenylenediamine) by resorcinol bis(diphenyl phosphate)] (RDP) and its implications on the thermomechanical processing, namely extrusion and injection molding, as well as on the thermal and mechanical properties of the formulations. This antiplasticization effect allows the processing of polyetherimide formulations at lower temperatures in comparison with neat polymer due to the progressive decrease of the glass transition temperature with increased RDP concentration, as observed by differential scanning calorimetry and dynamic mechanical analysis. The decrease of  $T_g$  occurs concomitantly with the overlap of the glass transition and  $\beta$  relaxation and with the shift of the  $\gamma$  relaxation to higher temperatures. These changes in the relaxation spectrum of polyetherimide formulations are possibly responsible for the increase of the tensile strength and Young's modulus and changes in the fracture mechanism, as observed by stress-strain tests and by scanning electron microscopy, respectively. © 2014 Wiley Periodicals, Inc. *J. Appl. Polym. Sci.* **2014**, *131*, 40619.

**KEYWORDS:** glass transition; mechanical properties; plasticizer; polyimides; synthesis and processing

Received 29 October 2013; accepted 18 February 2014

DOI: 10.1002/app.40619

## INTRODUCTION

Plasticizers are common additives of great interest for the engineering thermoplastics market, representing a third of the additives market.<sup>1</sup> The plasticization effect of low molar mass diluents mixed into polymeric materials is quite well known and topic of reviews and books.<sup>1–5</sup> The usual effect of plasticizers on a polymer matrix is characterized mainly by a decrease in the glass transition temperature ( $T_g$ ), Young's modulus, and tensile strength, with an increase in the elongation at break and toughness.<sup>1</sup> However, for some diluent-polymer pairs, an increase in stiffness is observed despite the usual decrease in glass transition temperature. This unexpected behavior is known as the antiplasticization effect<sup>6–10</sup> for which the magnitude depends on the molecular characteristics of the additives (size, shape, and stiffness), of the polymers (polarity and stiffness) and of the polymer-additives interactions.<sup>11,12</sup>

The antiplasticization occurs in many different diluent-polymer systems as, for example, tricresyl phosphate in polysulfone<sup>13,14</sup>; dibutylphthalate<sup>15,16</sup>; nonlinear optical dyes such as lead tetracumylphenoxy phthalocyanine<sup>17</sup> and *p*-terphenyl<sup>18</sup> in polycarbonate; phenacetin and acetanilide in poly(ethylene terephthalate)<sup>19</sup>; 4,4'-(hexafluoroisopropylidene) diphenol, hydroquinone, and 4-hydroxybenzophenone in poly(amino-ether) resin<sup>20</sup>; water in

starch<sup>21–23</sup>; water in poly(ether ether ketone)<sup>24</sup>; among others. The antiplasticization of poly(vinyl chloride) has been extensively studied for several diluents. For example, Kinjo and Nakagawa<sup>25</sup> studied the effect of five different diluents (tricresyl phosphate, butyl benzyl phthalate, dioctyl phthalate, dibutyl sebacate, and dioctyl sebacate) on the  $\beta$  secondary relaxation, glass transition, and Young's modulus, observing a simultaneous decrease in  $T_g$  and increase in modulus. The probable mechanism of antiplasticization is not well understood, however, the suppression of secondary relaxations with the decrease in  $T_g$ , together with changes in the free-volume, are considered as the main causes of it.<sup>10,19–30</sup> The antiplasticization magnitude is determined by the potential of the additive in inhibiting secondary relaxations.<sup>10</sup>

The antiplasticization induced by low molar mass molecules has been extensively used in order to improve the barrier properties of polymers. One argument for this is that antiplasticization is associated with losing of free volume that results in changes in the relaxation spectrum of the polymer and, therefore, in barrier and mechanical properties.<sup>20</sup> However, one of the most interesting aspects of this effect is the enhancement of the Young's modulus without losing the transparency of amorphous polymers, as the antiplasticizer is soluble in the polymer. Moreover,

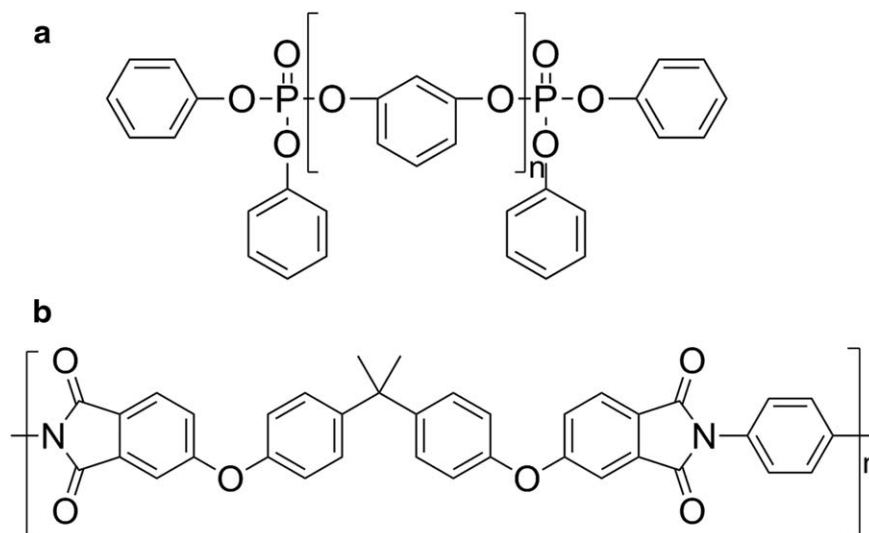


**Figure 1.** Chemical structure: (a) RDP and (b) poly(bisphenol A-*co*-4-nitrophthalic anhydride-*co*-1,3-phenylenediamine)—ULTEM® series 1000.

it allows the processing of high  $T_g$  polymers at lower temperatures (compared to neat). Indeed, from an industrial point of view this means saving energy during processing and simultaneously increasing mechanical performance among others properties.

According to Jackson and Caldwell<sup>12</sup> polymers which contain rigid and polar groups and stiff chains are likely to be antiplasticized. A polymer which presents these molecular characteristics and could be positively influenced by antiplasticization effect is the polyetherimide. Polyetherimide is an amorphous engineering thermoplastic presenting glass transition temperature of 215°C, reasonably high thermal stability and good mechanical properties for applications as sheets, rods, tubes, and other structural components.<sup>31,32</sup> However, this polymer must be processed at temperatures above 300°C to reach sufficiently low viscosity to allow the preparation of molded artifacts.<sup>33</sup>

Larocca and Pessan<sup>34</sup> reported the antiplasticization effect for four different additives [*N*-phenyl 2-naphthylamine (PNA), 4,4'-isopropylidene 2,6-di-bromophenol (TBBPA), 2,6-di-tert-butyl *p*-cresol (BHT), and 4,4'-hexafluor-isopropylidene-diphenol (HFBPA)] in poly(bisphenol A-*co*-4-nitrophthalic anhydride-*co*-1,3-phenylenediamine) membranes cast from chloroform solutions. Their analyses were focused on the mechanism of antiplasticization and its influence on gas permeation. Nevertheless, these additives are not suitable for thermomechanical processing because they are not thermally stable at temperatures above 250°C which is likely to be necessary for any polyetherimide-based formulations. An additive that can withstand this processing condition is tetraphenyl 1,3-phenylene bis(phosphate), known as resorcinol bis(diphenyl phosphate) or RDP.<sup>35</sup>

RDP is an aromatic phosphate commonly used as a flow modifier and flame retardant,<sup>35</sup> that shows higher thermal stability and lower volatility in comparison to previously reported poly-

etherimide additives.<sup>34</sup> Moreover, RDP presents some characteristics of antiplasticizers<sup>11</sup> such as polar and aromatic groups in its structure and  $T_g$  superior to  $-50^\circ\text{C}$ .

To our best knowledge, no literatures have reported the antiplasticization of polyetherimide by RDP. Therefore, the aim of this study is to report the antiplasticization effect of RDP on the injection molded polyetherimide formulations, describing its effect on  $T_g$ , processing temperature and on the mechanical properties of the formulations. With this aim, polyetherimide/RDP formulations were investigated using dynamic mechanical analyses, differential scanning calorimetry (DSC), thermogravimetric analyses, and stress-strain tests and the fractures were investigated by scanning electron microscopy (SEM).

## EXPERIMENTAL

### Materials

The commercial polyetherimide—ULTEM®1010 [(poly(bisphenol A-*co*-4-nitrophthalic anhydride-*co*-1,3-phenylenediamine))] was supplied by SABIC Innovative Plastics. The plasticizer RDP (Fyrolflex® RDP) supplied by Supresta presents about 60–75 wt % of dimer species and the rest are composed by other higher oligomers.<sup>35</sup> RDP is liquid at room temperature and presents glass transition at  $-33^\circ\text{C}$  (determined by DSC—result not shown) and specific volume of  $0.7704\text{ cm}^3\text{ g}^{-1}$  ( $25^\circ\text{C}$ ). The structures of the commercial polyetherimide and of RDP are shown in Figure 1.

### Sample Processing

The polyetherimide was previously milled. Premixtures of polyetherimide and RDP at concentrations of 3, 6, 9, 12, and 15 wt % were processed in a double screw mini compounder DSM Xplore at temperatures depending on the composition [from 330 to 280°C as shown in Figure 2(a)]. Tensile tests specimens (ASTM D1708) were injection molded using a micro injection molding machine DSM Xplore under a pressure of 8 bar and at temperatures from 340 to 240°C depending on compositions, as shown in Figure 2(a). The mold temperature was kept at 150°C.

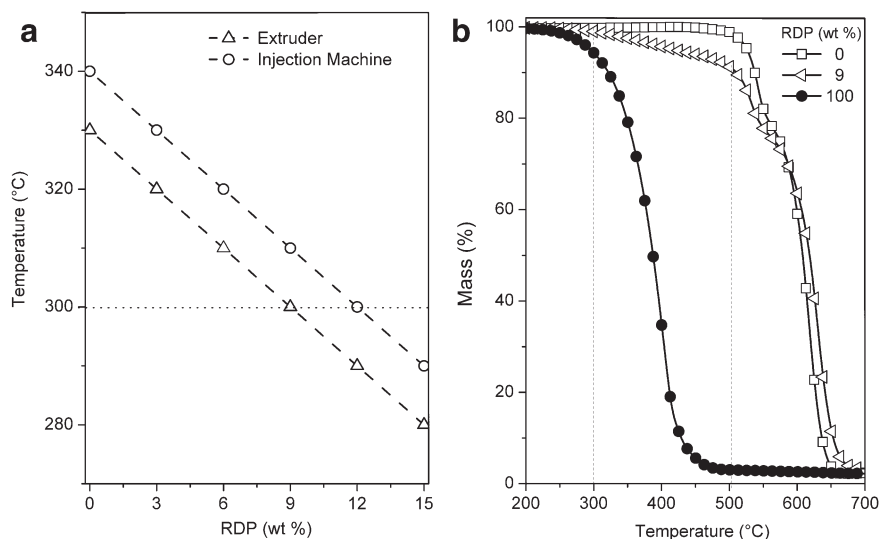


**Figure 2.** (a) Processing temperature (extrusion and injection molding) as functions of RDP concentration. (b) Thermogravimetric curves for polyetherimide, polyetherimide-9% RDP, and pure RDP.

### Characterization

Formulations were characterized by DSC using a MDSC—2910 TA Instruments equipment under an argon atmosphere, with an initial heating scan from 25 to 320°C at 20°C min<sup>-1</sup>, followed by a cooling scan from 320 to 25°C at 10°C min<sup>-1</sup> and a second heating scan from 25 to 320°C at 10°C min<sup>-1</sup>. Thermogravimetric analyses were performed on TGA 2050 equipment—TA-Instruments from 25 to 980°C at a heating rate of 10°C min<sup>-1</sup> under a constant synthetic air flow of 100 mL min<sup>-1</sup>. An oxidative atmosphere was used to provide better insights on possible thermal processes (oxidation, degradation etc.) during compounding. Dilatometric measurements were performed on a thermomechanical analyzer TMA 2940—TA Instruments at a heating rate of 5°C min<sup>-1</sup> from 0 to 250°C using cubic samples with side length of 3 mm cut from the central part of the tensile tests specimens. Dynamical-mechanical analyses (DMTA) were performed on a DMTA V equipment from Rheometric Scientific at a fixed frequency of 3 Hz. The samples (3.2 × 12.9 × 22 mm<sup>3</sup> dimensions) were cooled from room temperature to -150°C and then heated at 2°C min<sup>-1</sup> to 300°C, in single cantilever mode. The morphological characterization of the surface resulting from fractures in the tensile test was performed by SEM in a JEOL JSM6360-LV at 20 keV. The samples received a sputtered coating of gold in a Bal-Tec MD 020 Modular High Vacuum Coating System prior to the analysis.

### RESULTS AND DISCUSSION

The addition of RDP to polyetherimide allows a considerable decrease on the processing temperature. Although the neat polymer must be processed at 330°C to reach a sufficiently low viscosity for compounding and injection molding, the formulations could be processed at temperatures 10°C lower for each 3 wt % of RDP, reaching a processing temperature of 280°C for 15 wt % of RDP [Figure 2(a)]. Figure 2(b) shows the thermogravimetric curves under oxidative atmosphere for RDP, poly-

etherimide, and the formulation containing 9 wt % of RDP. The thermogravimetric curve for the polyetherimide presents two steps of mass loss at 500 and 550°C. The mechanism of the degradation of polyetherimides has been described in the literature. In principle, the thermal degradation results in chain random scission or crosslinking.<sup>36</sup> The random scission starts around 500°C and it results from the break of isopropylidene moieties, ether linkages and phenyl-phthalimide rings. This step is followed by other stage which produces CO<sub>2</sub> and water.<sup>37</sup> Conversely, Bright et al.<sup>35</sup> reported that RDP presents a mass loss of 0.3%; 0.8 and 3.0% after 2 min at 220, 250, and 280°C, respectively. Figure 2(b) shows that RDP presents 6 wt % of mass loss at 300°C (experiment performed at a heating rate of 10°C min<sup>-1</sup>), a thermal stability much higher than that of the previously mentioned additives, which degrade in the temperature range of 120 to 215°C.<sup>34</sup> Although for RDP mixed into polyetherimide the mass loss at 300°C is only 1%, as shown by the thermogravimetric curve for polyetherimide-9% RDP. The decrease of the mass loss of RDP incorporated to the polyetherimide matrix at 300°C can indicate that the RDP mass loss is controlled by the diffusion of the additive through the polyetherimide matrix.

Figure 2(a) shows that with RDP amounts higher than 9 wt % the compounding can be performed at temperatures below 300°C in the extruder. The injection machine barrel was set at higher temperatures in comparison with the extrusion conditions [Figure 2(a)]. However, in this processing step the mixture is exposed to such temperatures for short period of times (30 s) and under pressure (8 bar) and on these conditions significant changes in the RDP concentration is not expected. This hypothesis is confirmed by the thermogravimetric curve of polyetherimide-9% RDP, which shows a first mass loss of 9 wt % in the temperature range from 300 to 500°C [Figure 2(b)] due to the degradation and evaporation of RDP.

All polyetherimide/RDP formulations could be extruded and injection molded without significant composition changes,

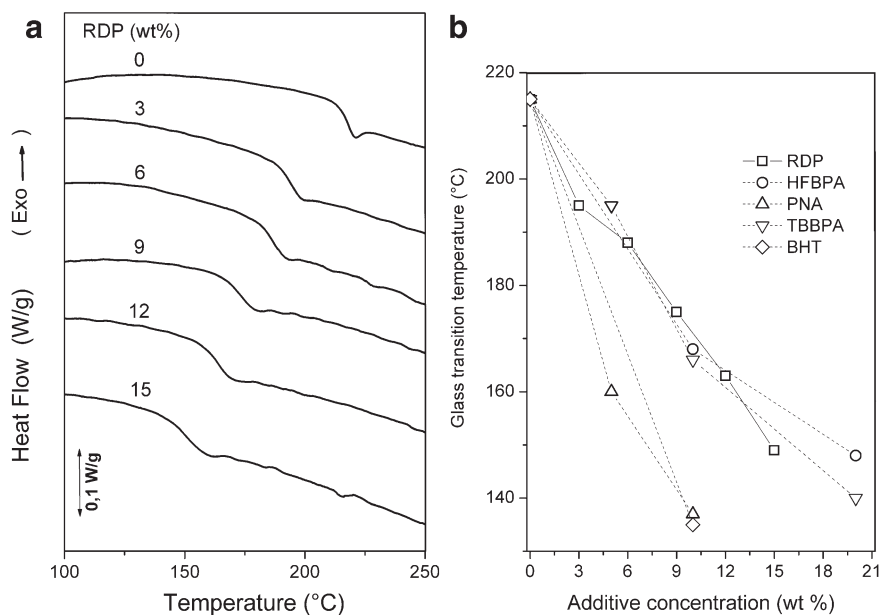


**Figure 3.** (a) DSC curves for polyetherimide/RDP formulations. (b)  $T_g$  of polyetherimide as a function of the concentration of RDP (our data) and HFBPA, PNA, TBBPA, and BHT from Ref. 34 (DSC data obtained at heating rate of  $20^\circ\text{C min}^{-1}$ ).

resulting in uniform and transparent specimens whose colors changes from ambar to brownish with increasing RDP concentration.

The mentioned decrease in the processing temperature is related to a decrease in  $T_g$ . Figure 3(a) shows the DSC curves corresponding to the second heating scan for the polyetherimide/RDP formulations (all DSC curves were normalized with respect to sample mass). The curves reveal a shift of the glass transition temperature ( $T_g$ ) from  $217^\circ\text{C}$  for neat polyetherimide to approximately  $149^\circ\text{C}$  for the composition with 15 wt % of RDP. The magnitude of this decrease is similar to the ones reported by Larocca and Pessan<sup>34</sup> for other additives, as shown in Figure 3(b).

The  $T_g$  and secondary relaxations of polyetherimide formulations were also investigated by DMTA and the results are shown in Figure 4. The loss modulus curves of the polyetherimide and its formulations [Figure 4(a)] reveal three relaxations ( $\alpha$  or glass transition,  $\beta$ , and  $\gamma$ ). The relaxations temperatures ( $T_g$ ,  $T_\beta$  and  $T_\gamma$ ) are taken as the temperature corresponding to the maximum of the relaxations peaks in the loss modulus curves and these data are shown in Table I. The  $\gamma$  transition, around  $-100^\circ\text{C}$ , is assigned to short distance relaxations involving a few segments of the polyetherimide backbone.<sup>38</sup> The  $\beta$  transition is a broad relaxation due to aromatic and benzimide groups,<sup>38</sup> starting around  $0^\circ\text{C}$ , being maximized at about  $100^\circ\text{C}$ . The peak in the loss modulus curve for polyetherimide related to the glass transition presents a maximum at  $240^\circ\text{C}$ . This peak is shifted to lower temperatures with increasing RDP content until it overlaps the  $\beta$  transition at a concentration of 12 wt % [Figure 4(a,b)]. The  $\gamma$  transition tends to be slightly shifted to higher temperatures with increasing amount of RDP, however, this effect is more evident at higher RDP contents. Figure 4(c) shows that the maximum

of the peak of the  $\gamma$  transition at  $-98^\circ\text{C}$  for neat polyetherimide is shifted to  $-90^\circ\text{C}$  for the formulation with 15 wt % of RDP. Despite the higher frequency (10 Hz) used in DMTA experiments, Larocca and Pessan<sup>34</sup> also reported shifts in the  $\gamma$  transition of this magnitude for amounts of low molar mass additives close to 15 wt %. Besides, a decrease of the damping factor ( $\tan \delta$ ) at  $T_\gamma$  with the addition of RDP in comparison with polyetherimide is observed [Figure 4(d)]. Damping factor is defined as the ratio of the loss modulus and storage modulus and the decrease of this parameter means that the capability of the formulations to dissipate energy is restrict. According to Robeson,<sup>10</sup> the decrease of the intensity of the  $\tan \delta$  is due to the restrictions of the secondary molecular relaxations. Similar behavior is observed for the polyetherimide/RDP formulations at  $25^\circ\text{C}$ , however, at  $T_g$  of each formulation the values of  $\tan \delta$  [Figure 4(d)] increase with the addition of RDP, what is expected because above  $T_g$  the formulations are in the liquid state and the RDP, a low molar mass additive, should contribute to the increase of the freedom degree of the macromolecules and of the free volume. These results suggest that the RDP influences the formation of the glassy state. The polyetherimide/RDP formulations were prepared by mechanical mixing in the melt in an extruder followed by injection molding. Thus, the glassy state is formed during cooling. The higher RDP amount the higher is the polymer chain mobility, what allows the chains to relax more during the cooling and the glass becomes denser. This hypothesis is reinforced by analyzing the results from dilatometry shown in Figure 5; the curves for polyetherimide and its formulation containing 9 wt % of RDP represent the relative expansion ( $\Delta L/L$ ) of the samples with increasing temperature. Both materials present similar dilatometric behavior in the glassy state, showing thermal expansion coefficient ( $\alpha$ ) of  $7.16 \times 10^{-5} \text{ }^\circ\text{C}^{-1}$  for polyetherimide and  $7.45 \times 10^{-5} \text{ }^\circ\text{C}^{-1}$  for the

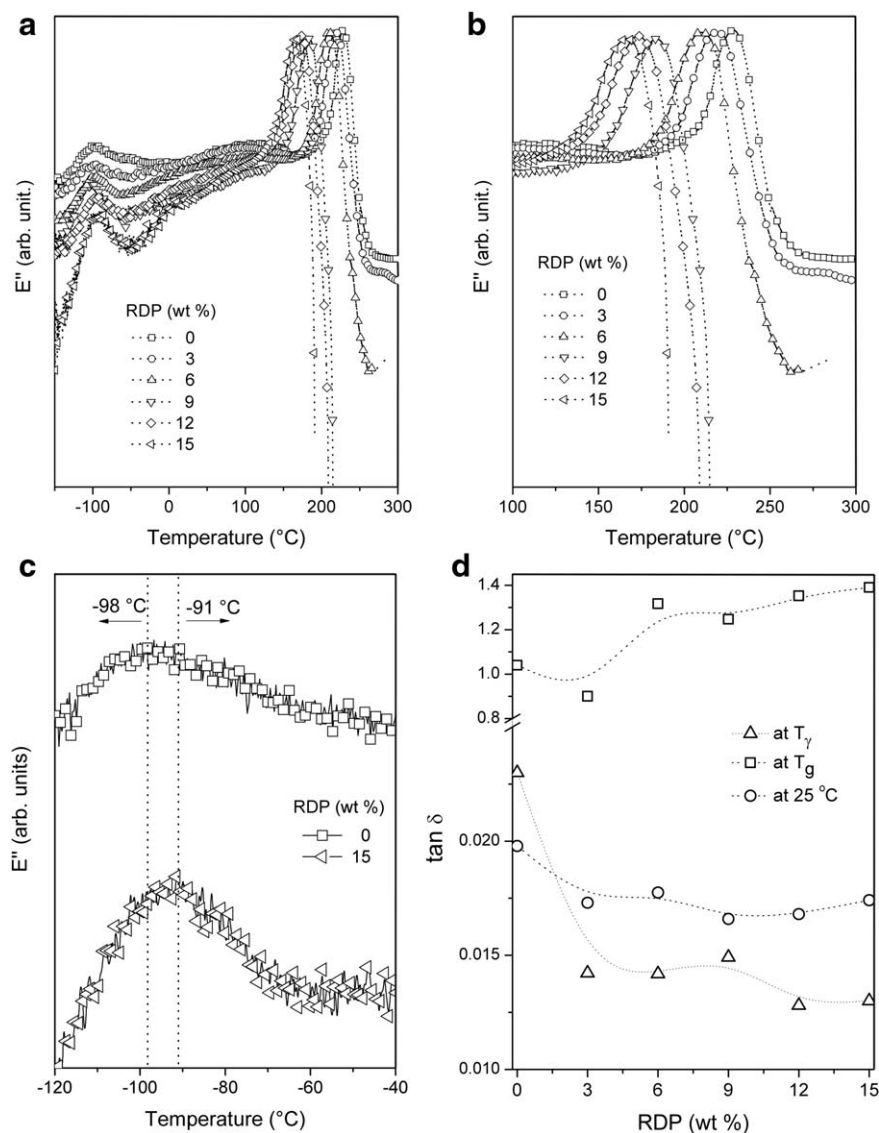


**Figure 4.** (a) and (b) loss modulus as a function of temperatures for neat polyetherimide and its formulation with RDP; (c) loss modulus at low temperatures for neat polyetherimide and polyetherimide with 15 wt % RDP, and (d)  $\tan \delta$  as a function of RDP concentration and at different temperatures.

plasticized sample. Close to the glass transition temperature a peak is observed in the curves due to shrinkage followed by expansion. The shrinkage is probable due to residual stress associated to the processing history of the samples and occurs

at temperatures in which the chains achieve mobility to enable the relaxations. The shrinkage is more intense for polyetherimide (120%) than for the formulation (65%) what means the glassy state of the formulation is nearer the equilibrium.

**Table I.** Glass Transition Temperature ( $T_g$ ) Determined from DSC and DMTA,  $T_\gamma$  and  $T_\beta$  Determined from DMTA, Young's Modulus, Strain at Break, and Tensile Strength as a Function of the RDP Contents

RDP (wt %)	$T_\gamma$ (°C)	$T_\beta$ (°C)	$T_g$ (°C)		Strain at break (%)	Young's modulus (MPa)	Tensile strength (MPa)
			DMTA	DSC			
0	-98	115	240	217	24 ± 5	970 ± 70	113 ± 1
3	-98	109	241	194	35 ± 12	1040 ± 30	119.2 ± 0.5
6	-95	113	224	187	20 ± 1	1050 ± 50	121 ± 1
9	-97	-	197	174	19 ± 1	1070 ± 30	123 ± 1
12	-93	-	190	163	31 ± 8	1120 ± 40	123.7 ± 0.7
15	-90	-	183	149	20 ± 3	1140 ± 30	124.2 ± 0.4



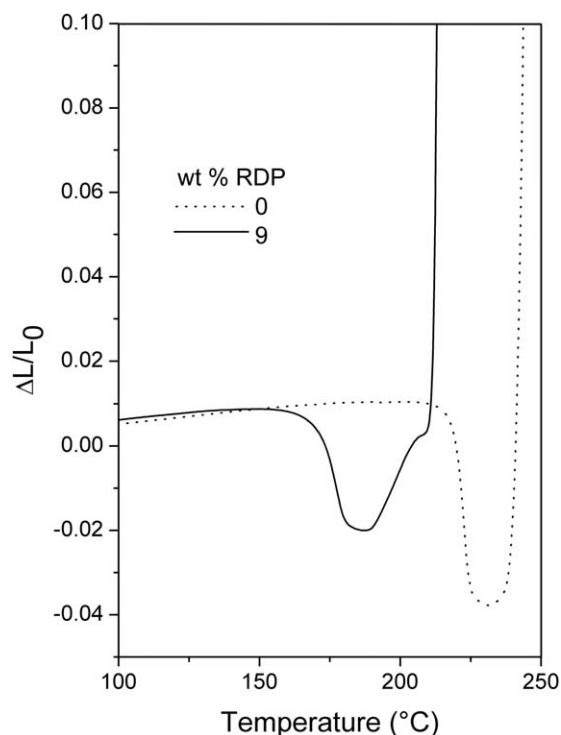


**Figure 5.** Dilatometric curves for neat polyetherimide and for the formulation with 9 wt % RDP.

According to Larocca and Pessan,<sup>34</sup> the changes of the relaxation spectrum of the polyetherimide with the addition of low molar mass additives is due to the restrictions on the secondary relaxations in the glassy state, as consequence of the decrease of the free volume of the polymer. Our results from DSC, dynamic mechanical analysis, and thermodilatometry strongly supports that RDP influences the formation of the glassy state of the formulations, leading to a reduction of the free volume in comparison with the neat polyetherimide.

The effect of RDP on the mechanical properties can be observed in the stress  $\times$  strain curves for polyetherimide-3% RDP and polyetherimide-9% RDP shown in Figure 6(a). It can be observed that the sample with 9 wt % of RDP has higher ultimate tensile strength while the elongation is not significantly changed (considering the standard deviation, both samples showed similar elongations). Table I and Figure 6(b) summarize the effect of RDP on the mechanical properties of the formulations. As mentioned in Introduction, for a plasticized material a decrease in  $T_g$  results in lower modulus and strength, as the molecules would have higher mobility and lower interaction with each other. Nevertheless, an increase in both parameters with increased amount of RDP is observed, with the tensile strength going from  $(113 \pm 1)$  MPa to  $(124.2 \pm 0.4)$  MPa and the Young's modulus from  $(970 \pm 70)$  MPa to  $(1130 \pm 30)$  MPa, for the neat and the 15 wt % RDP samples, respectively. This represents an increase of 10% in tensile strength and 16% in Young's modulus. Similar stiffening effect was reported by Larocca and Pessan<sup>34</sup> for formulations of polyetherimide/low molar mass additives. The observed increase in these properties together with the lowering of the glass transition temperature with increasing RDP concentration demonstrates the antiplasticization effect of RDP on polyetherimide.

The RDP antiplasticizer effect on polyetherimide plays an important role on the fracture morphology of the formulations. The fractures of the polyetherimide and its formulations with 6 and 12 wt % of RDP, resulting from the break of the sample subjected to tensile tests show conic markings (Figure 7).

The micromechanism of dynamic fracture is governed by nucleation, growth and coalescence of microcracks, and the fracture patterns is directly related to the mechanism of crack propagation.<sup>39–42</sup> For example, the conic markings, that include parabolas, ellipses, and circles, result from the intersection of a moving primary or main planar crack front and a secondary crack front, which grows radially (Type I) and also from the intersection of two secondary cracks (Type II).<sup>41</sup> Wenbo and Tingqing<sup>40</sup> and

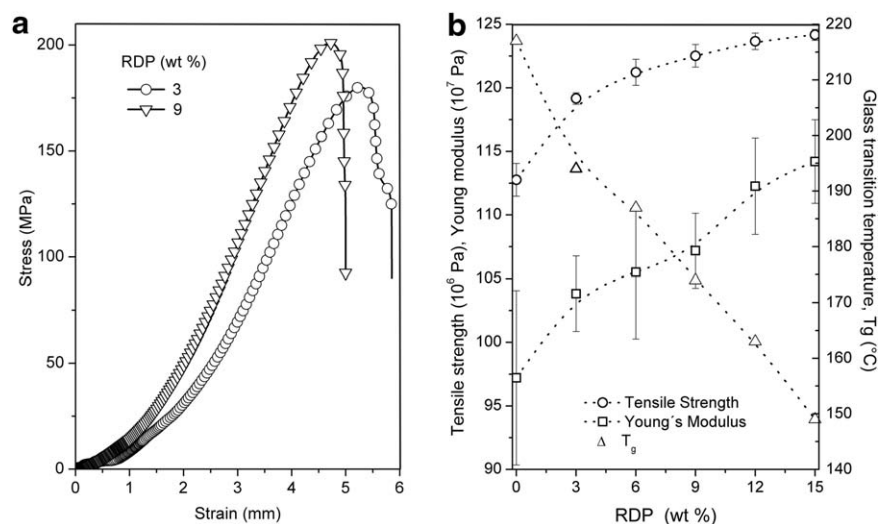


**Figure 6.** (a) Typical stress–strain curve for polyetherimide plasticized with 3 and 9 wt % RDP; (b) tensile strength, Young's modulus, and glass transition temperature as a function of RDP content.

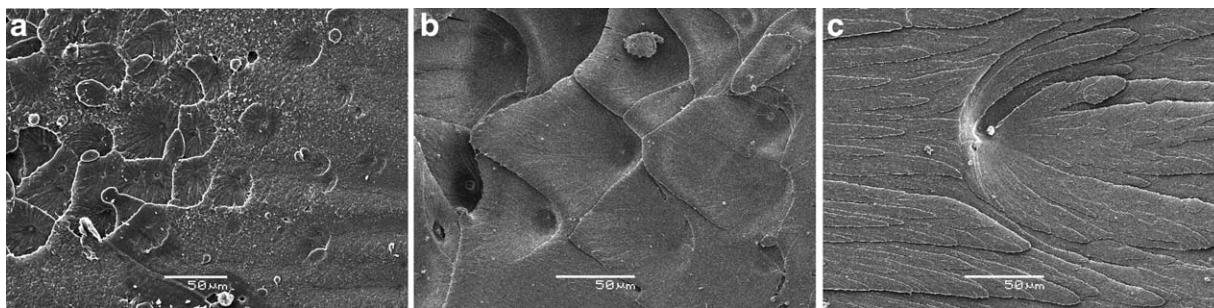


**Figure 7.** SEM micrographs of surfaces resulting from fractures of the tensile tests: (a) neat polyetherimide, polyetherimide containing (b) 6 wt %, and (c) 12 wt % RDP.

Zheng and coworkers<sup>41</sup> studied the effects of the velocity ratio of the main crack ( $V_m$ ) to the secondary crack ( $V_s$ ) on the fracture surface morphology using computer simulations and found out that the morphology can change from parabolas to ellipses and circles by increasing  $V_m/V_s$  ratio. The number of the conic markings is determined by the secondary cracks initiation.

The analysis of the morphology of the fractures shown in Figure 7 reveals a decrease of the number and an increase of the size of the conic markings with increasing RDP amount. Moreover, for neat polyetherimide and polyetherimide containing 6 wt % of RDP the Type II conic markings are predominant indicating an intense secondary cracks initiation. The crack initiation sites can be micro heterogeneities such as impurities, microvoids, residual stress, and density fluctuations,<sup>41</sup> for instance. As discussed above, the dilatometric experiments provided evidences of the residual stress in the specimens produced by mechanical processing. Moreover, the residual stress seems to decrease as the amount of RDP increases. A possible explanation for the changes in the fracture patterns is the residual stress of the specimens; however, a more detailed study should be conducted to understand completely the fracture mechanism of these formulations.

The results clearly show that RDP produces an antiplasticization effect on polyetherimide injection molded formulations. This effect has interesting technological implications for the manufacturing of polyetherimide-based components, from an industrial point of view. The processing temperature can be reduced from 330 to 280°C what represents a considerable decrease in energy consumption in a large scale production. Besides its common use as flow modifier and flame retardant,<sup>35</sup> RDP improves the stiffness and strength of the polyetherimide and does not degrade or volatilize significantly in the processing conditions. The only drawback is if one intends to use polyetherimide-based components at higher temperatures, as the  $T_g$  is considerably decreased. Nevertheless, for room temperature applications, the methodology described herein presents many advantages for the production of injection molded polyetherimide components.

## CONCLUSIONS

RDP produces an antiplasticization effect on molded polyetherimide specimens, which is characterized by a progressive decrease of the processing temperature and of the  $T_g$ , together

with an increase of the tensile strength and Young's modulus, respectively, with increased amount of additive. The thermal stability of polyetherimide in the processing temperature range is not considerably influenced by RDP addition, as the loss of this additive at the temperature range of extrusion and injection molding is not significant. The study here developed is of relevant importance for industrial applications for polyetherimide, providing a decrease in energy consumption with an improvement in mechanical properties and is an interesting strategy against the high temperatures needed for processing of polyetherimide.

## ACKNOWLEDGMENTS

The authors thank Prof. C.H. Collins for manuscript revision, FAPESP for financial support (2010/02098-0 e 2010/17804-7) and fellowships (2010/03383-0 and 2010/18268-1) and SABIC Innovative Plastics for supplying polyetherimide and RDP.

## REFERENCES

1. Rahman, M.; Brazel C. S. *Prog. Polym. Sci.* **2004**, *29*, 1223.
2. Rosen, S. L. *Fundamental Principles of Polymeric Materials*; Wiley: New York, **1993**; p 97.
3. Wypych, G. *Handbook of Plasticizers*; Chem Tech Publishers: New York, **2004**.
4. Vieira, M. G. A.; Silva, M. A.; Santos, L. O.; Beppu, M. M. *Eur. Polym. J.* **2011**, *47*, 254.
5. Craver, C. D.; Carraher C. E. *Applied Polymer Science: 21st Century*; Elsevier: London, **2005**; Chapter 9, pp 157–176.
6. Stukalin, E. B.; Douglas, J. F.; Freed K. F. *J. Chem. Phys.* **2010**, *132*, 84504.
7. Anderson, S. L.; Grulke, E. A.; DeLassus, P. T.; Smith, P. B.; Kocher, C. W.; Landes, B. G. *Macromolecules* **1995**, *28*, 2944.
8. Riggelman, R. A.; Douglas, J. F.; Pablo, J. J. *Soft Matter* **2010**, *6*, 292.
9. Riggelman, R. A.; Douglas, J. F.; Pablo, J. J. *J. Chem. Phys.* **2007**, *126*, 234903.
10. Robeson, L. M. *Polym. Eng. Sci.* **1969**, *9*, 277.
11. Jackson, J. W.; Caldwell, J. R. *J. Appl. Polym. Sci.* **1967**, *11*, 211.
12. Jackson, J. W.; Caldwell, J. R. *J. Appl. Polym. Sci.* **1967**, *11*, 227.

13. Maeda, Y.; Paul, D. R. *J. Polym. Sci. B: Polym. Phys.* **1987**, *25*, 957.
14. Ventras, J. S.; Duda, J. L.; Ling, H. C. *Macromolecules* **1988**, *21*, 1470.
15. Liu, Y.; Roy, A. K.; Jones, A. A.; Inglefield, P. T.; Ogden, P. *Macromolecules* **1990**, *23*, 968.
16. Belfiore, L. A.; Henrichs, P. M.; Massa, D. J.; Zumbulyadis, N.; Rothwell, W. P.; Cooper, S. L. *Macromolecules* **1983**, *16*, 1744.
17. Ranade, A.; Wang, H.; Hiltner, A.; Baer, E.; Shirk, J. S.; Lepkowitz, R. S. *Polymer* **2003**, *48*, 624.
18. Miyagawa, A.; Korkiatithaweechai, S.; Nobukawa, S.; Yamaguchi, M. *Ind. Eng. Chem. Res.* **2013**, *52*, 5048.
19. Lee, J. S.; Leisen, J.; Choudhury, R. P.; Kriegel, R. M.; Beckham, H. W.; Koros, W. J. *Polymer* **2012**, *53*, 213.
20. Eceolazza, S.; Iriarte, M.; Uriarte, C.; Del Rio J.; Etxeberria, A. *Eur. Polym. J.* **2012**, *48*, 1218.
21. Pittia, P.; Sacchetti, G. *Food Chem.* **2008**, *106*, 1417.
22. Chang, Y. P.; Cheah, P. B.; Seow, C. C. *J. Food Sci.* **2000**, *65*, 445.
23. Chang, Y. P.; Karim, A. A.; Seow, C. C. *Food Hydrocoll.* **2005**, *20*, 1.
24. Iqbal, T.; Briscoe, B. J.; Luckham, P. F. *Eur. Polym. J.* **2011**, *47*, 2244.
25. Kinjo, N.; Nakagawa, T. *Polym. J.* **1973**, *4*, 143.
26. Guerrero, S. J. *Macromolecules* **1989**, *22*, 3480.
27. Ghersa, P. *Mod. Plast.* **1958**, *36*, 135.
28. Duda, J. L.; Romdhane, I. H.; Danner, R. P. *J. Non-Cryst. Solids* **1994**, *172–174*, 715.
29. Ngai, K.; Rendell, R. W.; Yee, A. F.; Plazek, D. J. *Macromolecules* **1991**, *24*, 61.
30. Rizos, A. K.; Petihakis, L.; Ngai, K. L.; Wu, J.; Yee, A. F. *Macromolecules* **1999**, *32*, 7921.
31. Belana, J.; Cañadas, J. C.; Diego, J. A.; Mudarra, M.; Díaz-Calleja, R.; Friederichs, S.; Jaimes, C.; Sanchis, M. *J. Polym. Intern.* **1998**, *48*, 11.
32. Tan, L.-S. In *Polymer Data Handbook*; Mark, J. E., Ed.; Oxford University Press, Inc.: New York, **1999**; pp 471–478.
33. Siochi, E. J.; Working, D. C.; Park, C.; Lillehei, P. T.; Rouse J. H.; Topping, C. C.; Bhattacharyya, A. R.; Kumar S. *Composites B* **2004**, *3*, 439.
34. Larocca, N. M.; Pessan, L. A. *J. Membr. Sci.* **2003**, *218*, 69.
35. Bright, D. A.; Dashevsky, S.; Moy, P. Y.; Williams, B. J. *Vinyl Addit. Technol.* **1997**, *3*, 170.
36. Caroccio, S.; Puglisi, C.; Montaudo, G. *Macromol. Chem. Phys.* **1999**, *200*, 2345.
37. Amancio-Filho, S. T.; Roeder, J.; Nunes, S. P.; dos Santos, J. F.; Beckmann, F. *Polym. Degrad. Stab.* **2008**, *93*, 1529.
38. Jenkins, M. J. *Polymer* **2000**, *41*, 6803.
39. Ravi-Chandar, K.; Yang, B. *J. Mech. Phys. Solids* **1997**, *45*, 535.
40. Wenbo, L.; Tingqing Y. *J. Appl. Polym. Sci.* **2003**, *89*, 1722.
41. Du, P.; Xue, B.; Song, Y.; Lu, S.; Zheng, Q.; Yu, J. *J. Mater. Sci.* **2010**, *45*, 3088.
42. Ravi-Chandar, K. *Dynamic Fracture*; Elsevier: Amsterdam, **2004**.